

Search for narrow resonances below the Υ mesons

The CDF collaboration

(Dated: July 21, 2008)

Abstract

We report a search for narrow resonances that decay into muon pairs in the invariant mass range $6.3 - 9.0 \text{ GeV}/c^2$. The data, collected by the CDF II experiment at the Fermilab Tevatron collider, correspond to an integrated luminosity of 630 pb^{-1} . We set 90% upper credible limits at about 1% on R , the ratio of the production cross section times muonic branching fraction of possible narrow resonances to that of the $\Upsilon(1S)$ meson.

PACS numbers: 13.20.Gd, 13.60.Le

I. INTRODUCTION

Searches for narrow resonances at SPEAR have set upper bounds on Γ_l , the leptonic width of possible resonances, of 100 eV in the mass region $5.7 \leq E_{\text{cm}} \leq 6.4$ GeV and of approximately 60 eV in the region $7.0 \leq E_{\text{cm}} \leq 7.4$ GeV [1]. These limits do not exclude bound states of light charge $-1/3$ spin -0 quarks the existence of which is required by supersymmetric theories. The leptonic width of \mathcal{E} mesons, 1^{--} bound states of charge $-1/3$ scalar quarks, has been evaluated in Ref. [2] using potential models of ordinary heavy quarks [3]. Because of the p-wave suppression of the fermion contribution to their decay width, the leptonic width is estimated to be approximately 18 (6) eV for a resonance with a 6 (10) GeV/ c^2 mass. A more recent study [4] has set an average 90% upper credible limit of $\Gamma_l \simeq 8$ eV to the existence of narrow resonances in the invariant mass range $6.3 - 9$ GeV/ c^2 by using muon pairs from a dataset corresponding to approximately 110 pb^{-1} collected with the CDF detector during the 1992-1995 Tevatron collider run.

However, because of statistical fluctuations, that study does not rule out the existence of \mathcal{E} states over the full mass range. In particular, at a mass of $7.2 \text{ GeV}/c^2$ that study returns an anomalously large upper credible limit that is consistent with what is expected if an \mathcal{E} state is produced.

This paper repeats the study in Ref [4] taking advantage of a higher statistics data sample that corresponds to an integrated luminosity of 630 pb^{-1} collected with the CDF II detector after may 2006. At that time, the CDF II trigger system has been upgraded and is capable of acquiring events containing muon pairs with invariant mass larger than $6 \text{ GeV}/c^2$ with a kinematical acceptance comparable to that of the Run I trigger system. Section II describes the detector systems relevant to this analysis. The data sample and analysis method are described in Sec. III. In Sec. IV, we fit the dimuon invariant mass distribution and derive 90% upper credible limits to Γ_l as a function of the resonance mass. Our conclusions are summarized in Sec. V.

II. CDF II DETECTOR AND TRIGGER SYSTEM

CDF II is a multipurpose detector, equipped with a charged particle spectrometer and a finely segmented calorimeter. In this section, we describe the detector components that are

relevant to this analysis. The description of these subsystems can be found in Refs. [5–14]. Two devices inside the 1.4 T solenoid are used for measuring the momentum of charged particles: the silicon vertex detector (SVXII and ISL) and the central tracking chamber (COT). The SVXII detector consists of microstrip sensors arranged in six cylindrical shells with radii between 1.5 and 10.6 cm, and with a total z coverage ¹ of 90 cm. The first SVXII layer, also referred to as L00 detector, is made of single-sided sensors mounted on the beryllium beam pipe. The remaining five SVXII layers are made of double-sided sensors and are divided into three contiguous five-layer sections along the beam direction z . The two additional silicon layers of the ISL help to link tracks in the COT to hits in the SVXII. The COT is a cylindrical drift chamber containing 96 sense wire layers grouped into eight alternating superlayers of axial and stereo wires. Its active volume covers $|z| \leq 155$ cm and 40 to 140 cm in radius. The transverse momentum resolution of tracks reconstructed using COT hits is $\sigma(p_T)/p_T^2 \simeq 0.0017$ [GeV/c]⁻¹. COT tracks are extrapolated into the SVXII detector and refitted adding hits consistent with the track extrapolation.

The central muon detector (CMU) is located around the central electromagnetic and hadronic calorimeters, which have a thickness of 5.5 interaction lengths at normal incidence. The CMU detector covers a nominal pseudorapidity range $|\eta| \leq 0.63$ relative to the center of the detector, and is segmented into two barrels of 24 modules, each covering 15° in ϕ . Every module is further segmented into three submodules, each covering 4.2° in ϕ and consisting of four layers of drift chambers. The smallest drift unit, called a stack, covers a 1.2° angle in ϕ . Adjacent pairs of stacks are combined together into a tower. A track segment (hits in two out of four layers of a stack) detected in a tower is referred to as a CMU stub. A second set of muon drift chambers (CMP) is located behind an additional steel absorber of 3.3 interaction lengths. The chambers are 640 cm long and are arranged axially to form a box around the central detector. The CMP detector covers a nominal pseudorapidity range $|\eta| \leq 0.54$ relative to the center of the detector. Muons which produce a stub in both CMU and CMP systems are called CMUP muons. The CMX muon detector consists of four drift chambers layers and scintillation counters positioned behind the hadron calorimeter. The

¹ In the CDF coordinate system, θ and ϕ are the polar and azimuthal angles of a track, respectively, defined with respect to the proton beam direction, z . The pseudorapidity η is defined as $-\log \tan(\theta/2)$. The transverse momentum of a particle is $p_T = p \sin(\theta)$. The rapidity is defined as $y = 1/2 \cdot \log((E + p_z)/(E - p_z))$, where E and p_z are the energy and longitudinal momentum of the particle associated with the track.

CMX detector extends the muon coverage to $|\eta| \leq 1$.

The luminosity is measured using gaseous Cherenkov counters (CLC) that monitor the rate of inelastic $p\bar{p}$ collisions. The inelastic $p\bar{p}$ cross section at $\sqrt{s} = 1960$ GeV is scaled from measurements at $\sqrt{s} = 1800$ GeV using the calculations in Ref. [15]. The integrated luminosity is determined with a 6% systematic uncertainty [16].

CDF uses a three-level trigger system. At Level 1 (L1), data from every beam crossing are stored in a pipeline capable of buffering data from 42 beam crossings. The L1 trigger either rejects events or copies them into one of the four Level 2 (L2) buffers. Events that pass the L1 and L2 selection criteria are sent to the Level 3 (L3) trigger, a cluster of computers running speed-optimized reconstruction code.

For this study, we select events with two muon candidates identified by the L1 and L2 triggers. The L1 trigger uses tracks with $p_T \geq 1.5$ GeV/c found by a fast track processor (XFT). The XFT examines COT hits from the four axial superlayers and provides $r - \phi$ information. The XFT finds tracks with $p_T \geq 1.5$ GeV/c in azimuthal sections of 1.25° . The XFT passes the tracks to a set of extrapolation units that determine the CMU (CMX) towers in which a CMU (CMX) stub should be found if the track is a muon. If a stub is found, a L1 CMU (CMX) primitive is generated. The L1 dimuon trigger requires one CMU primitive and an additional CMU or CMX primitive. The L2 trigger additionally requires that at least one of the muons has a CMUP stub matched to an XFT track with $p_T \geq 3$ GeV/c and that additional CMU (CMX) stubs are matched to XFT tracks with $p_T \geq 1.5$ (2) GeV/c. The L2 trigger is prescaled at high luminosity with a prescale factor that is dynamically chosen to optimize overall data acquisition performances.

The L3 trigger selects muon pairs with invariant mass larger than 5 GeV/c², and $|\delta z_0| \leq 5$ cm, where z_0 is the z coordinate of the muon track at its point of closest approach to the beam line in the $r - \phi$ plane. These requirements define the dimuon trigger used in this analysis.

III. DIMUON DATA SAMPLE

In this analysis, we select events acquired with the dimuon trigger and which contain two and only two muons with opposite charge. Events are reconstructed offline taking advantage of more refined calibration constants and reconstruction algorithms. COT tracks

are extrapolated into the SVXII detector, and refitted adding hits consistent with the track extrapolation. We require that at least one muon has stubs reconstructed in both the CMU and CMP detectors and matched to tracks with $p_T \geq 3$ GeV/ c . A track is identified as a CMUP muon if $\Delta r\phi$, the distance in the $r - \phi$ plane between the track projected to the CMU (CMP) chambers and a CMU (CMP) stub, is less than 30 (40) cm. The additional muon is accepted if a stub reconstructed in the CMU or CMX detectors is matched to a track with $p_T \geq 2$ GeV/ c . A track is identified as a CMU (CMX) muon if $\Delta r\phi$ is less than 30 (50) cm. We require that muon-candidate stubs correspond to L1 primitives, and correct the muon momentum for energy losses in the detector. Previous measurements of the B hadron mixing probability [17] and of the $b\bar{b}$ correlated production [18] have used similarly selected dimuon data samples. Those studies show that 70 – 75% of these dimuon pairs are contributed by $b\bar{b}$ and $c\bar{c}$ production. Following Ref. [4], we reject muons arising from the decay of hadrons with heavy flavor with the following requirements:

1. Isolation. The isolation, I , is defined as the scalar sum of the transverse momenta of all the tracks in a cone of radius $R = \sqrt{\delta\phi^2 + \delta\eta^2} = 0.4$ around the muon direction. We require that both muons have isolation $I \leq 4$ GeV/ c .
2. Promptness. In contrast to b and c -hadrons, the $\Upsilon(1S)$ and \mathcal{E} mesons have negligible lifetime. We evaluate the invariant mass of each muon pair by constraining the two muon tracks to originate from a common point in the three-dimensional space (vertex constraint). We reject muon pairs if the probability of the vertex constrained fit is smaller than 0.001. We also reject muon pairs if $L_{xy}/\sigma_{L_{xy}} \geq 3$, where L_{xy} is the displacement of the dimuon-candidate vertex with respect to the primary event vertex projected onto the dimuon transverse momentum vector, and $\sigma_{L_{xy}}$ is its uncertainty.

The invariant mass distribution of the muon pairs passing our selection cuts is shown in Fig. 1.

IV. SEARCH FOR NARROW RESONANCES

As in Ref. [4], we limit our search for narrow resonances to the mass region above 6.3 GeV/ c^2 at which the kinematical acceptance becomes independent of the \mathcal{E} -candidate transverse momentum. The number of Υ mesons in the data is derived by fitting the invari-

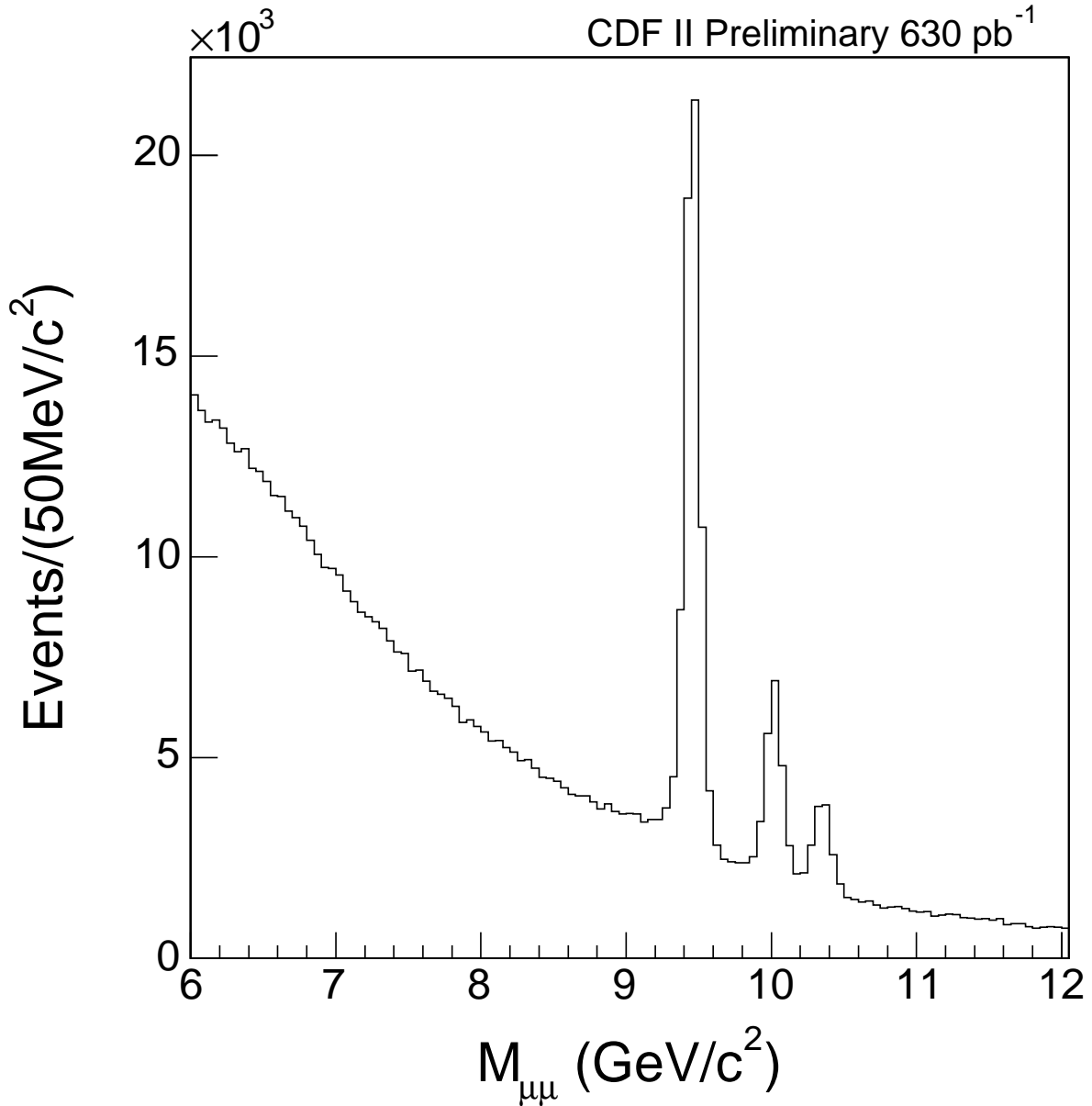


FIG. 1: Invariant mass distribution of the selected muon pairs.

ant mass distribution in Fig. 1 with a binned maximum likelihood method [19]. We use a fifth order polynomial to model the continuum in the invariant mass region 6 – 12 GeV/c^2 and Gaussian functions to model the Υ contributions². The best fit returns 52700 ± 350 $\Upsilon(1S)$ mesons events. The fit also returns $M_{\Upsilon(1S)} = 9459 \pm 1$ MeV/c^2 and a mass resolution

² Two Gaussian functions are used to model the $\Upsilon(1S)$ and the $\Upsilon(2S)$ peaks, while a single Gaussian function is used to model the $\Upsilon(3S)$ peak.

$\sigma_M = 52 \pm 1 \text{ MeV}/c^2$. This mass resolution is well modeled by a simulation of the process $p\bar{p} \rightarrow \Upsilon(1S)X$. In the simulation, the event generator produces unpolarized $\Upsilon(1S)$ mesons with the transverse momentum distribution of the data [20] and a flat rapidity distribution for $|y| \leq 1$. The generated events are processed with the CDF II detector simulation that in turn is based on the GEANT simulation package [21]. Events are then required to pass the same selection and reconstruction criteria imposed on the data. The same simulation ³ predicts an invariant mass resolution that increases from $32 \text{ MeV}/c^2$ for a \mathcal{E} state with a mass of $6.3 \text{ GeV}/c^2$ to $50 \text{ MeV}/c^2$ for $m_{\mathcal{E}} = 9 \text{ GeV}/c^2$.

We do not find any significant excess and we proceed to set limits. We set limits on $\sigma \cdot B$ relative to $\Upsilon(1S)$ with the following assumptions:

- the resonance has a width below the experimental resolution;
- the resonance is produced unpolarized;
- the resonance is produced with small associated activity.

This last assumption is necessary in order to use the isolation selection to improve purity of the data. The limits are set assuming near 100% efficiency for isolation as measured for $\Upsilon(1S)$. For example production mechanisms where the searched resonance is produced inside a jet, would correspond to lower isolation efficiency and higher limits that are not accounted for in this paper.

In order to set limits on the existence of narrow \mathcal{E} states we add a Gaussian term to the likelihood function and fit the data in the $6-9.1 \text{ GeV}/c^2$ mass interval. We perform 108 fits, in which we change the position of the Gaussian peak in steps of $25 \text{ MeV}/c^2$ from 6.3 to $9.0 \text{ GeV}/c^2$. In each fit, we force the Gaussian width to the RMS mass resolution predicted by the detector simulation for that mass. Since we are using a single Gaussian to model the \mathcal{E} signal, while two Gaussian functions are used to model the reference $\Upsilon(1S)$ peak there could be a small systematic effect that does not cancel in the ratio. This effect is estimated to be smaller than the contribution of the second Gaussian of the reference $\Upsilon(1S)$ peak which

³ When simulating \mathcal{E} states, the transverse momentum distribution is rescaled from that of the $\Upsilon(1S)$ data so that $\langle p_T^{\mathcal{E}} \rangle / \langle p_T^{\Upsilon(1S)} \rangle = m_{\mathcal{E}}/m_{\Upsilon(1S)}$. For J/ψ mesons, this rescaling procedure predicts a $d\sigma/dp_T$ distribution that decreases more rapidly with increasing momenta than the distribution of the data. However, a poor modeling of the transverse momentum distribution is not a cause of error because the kinematic acceptance does not depend on the \mathcal{E} transverse momentum within a couple of percents.

is 4.5%. In order to account for it, we add a 4.5% systematics to the limit. For each mass peak, we use the integral of the Gaussian function, and its error, returned by the best fit to derive N_{ul} , the 90% credibility upper limit to the number of events contributed by a narrow resonance ⁴. We evaluate the ratio of the geometric and kinematic acceptance for an \mathcal{E} resonance to that for the $\Upsilon(1S)$ meson with the above described simulation. The geometric and kinematic acceptance depends on the resonance mass and increases from 65.5% of that of the $\Upsilon(1S)$ meson for $m_{\mathcal{E}} = 6.3 \text{ GeV}/c^2$ to 97.4% for $m_{\mathcal{E}} = 9.0 \text{ GeV}/c^2$. Small data-to-simulation correction factors for the trigger and reconstruction efficiency [18, 22] depend little on the muon p_T and are neglected as in the study in Ref. [4]. The acceptance of the reference $\Upsilon(1S)$ meson depends on $\Upsilon(1S)$ polarization. If the $\Upsilon(1S)$ has maximum longitudinal polarization the acceptance $\Upsilon(1S)$ goes up by 5%, on the contrary if it has maximum transverse polarization it goes down by 3%. Given the current measurements of $\Upsilon(1S)$ polarization at the Tevatron [23, 24] we add a 3% systematic to account for this effect. The total systematic on the limit is then 6%.

The ratio of N_{ul} to the number of observed $\Upsilon(1S)$ mesons, corrected for the relative acceptance, is the 90% credibility upper limit to $R = \sigma_{\mathcal{E}} B(\mathcal{E} \rightarrow \mu\mu)/\sigma_{\Upsilon(1S)} B(\Upsilon(1S) \rightarrow \mu\mu)$. These limits are plotted in Fig. 2 as a function of the \mathcal{E} mass. Figure 3 shows the 90% upper credible limits to $\Gamma_l^{\mathcal{E}}$. These limits are derived under the assumption ⁵ that $\sigma_{\mathcal{E}} = \sigma_{\Upsilon(1S)} \times (m_{\Upsilon(1S)}/m_{\mathcal{E}})^3 \times \Gamma_{\mu}^{\mathcal{E}}/\Gamma_{\mu}^{\Upsilon(1S)}$ [4]. The two figures also show in blue the limit with systematics included, and the expected limit in red⁶

V. CONCLUSIONS

We have investigated the invariant mass spectrum of muons pairs, produced at the Fermilab Tevatron collider and collected by the CDF experiment, and improve previous limits to the existence of narrow resonances in the invariant mass range 6.3 – 9.0 GeV/ c^2 . We derive

⁴ The integral of the fit likelihood from N_{ul} to infinity is 2% of the integral of the fit likelihood from 0 to infinity. The justification for this procedure is Bayesian with a prior that is zero for negative resonance cross sections and flat for positive ones.

⁵ As noted in Ref. [4], this equation tends to underestimate the production cross section of states lighter than the $\Upsilon(1S)$ meson. In that was the case, the $\Gamma_l^{\mathcal{E}}$ limits set by our study would be correspondingly smaller than those indicated in Fig. 3.

⁶ The expected limit is derived assuming the fit returns 0 ε events.

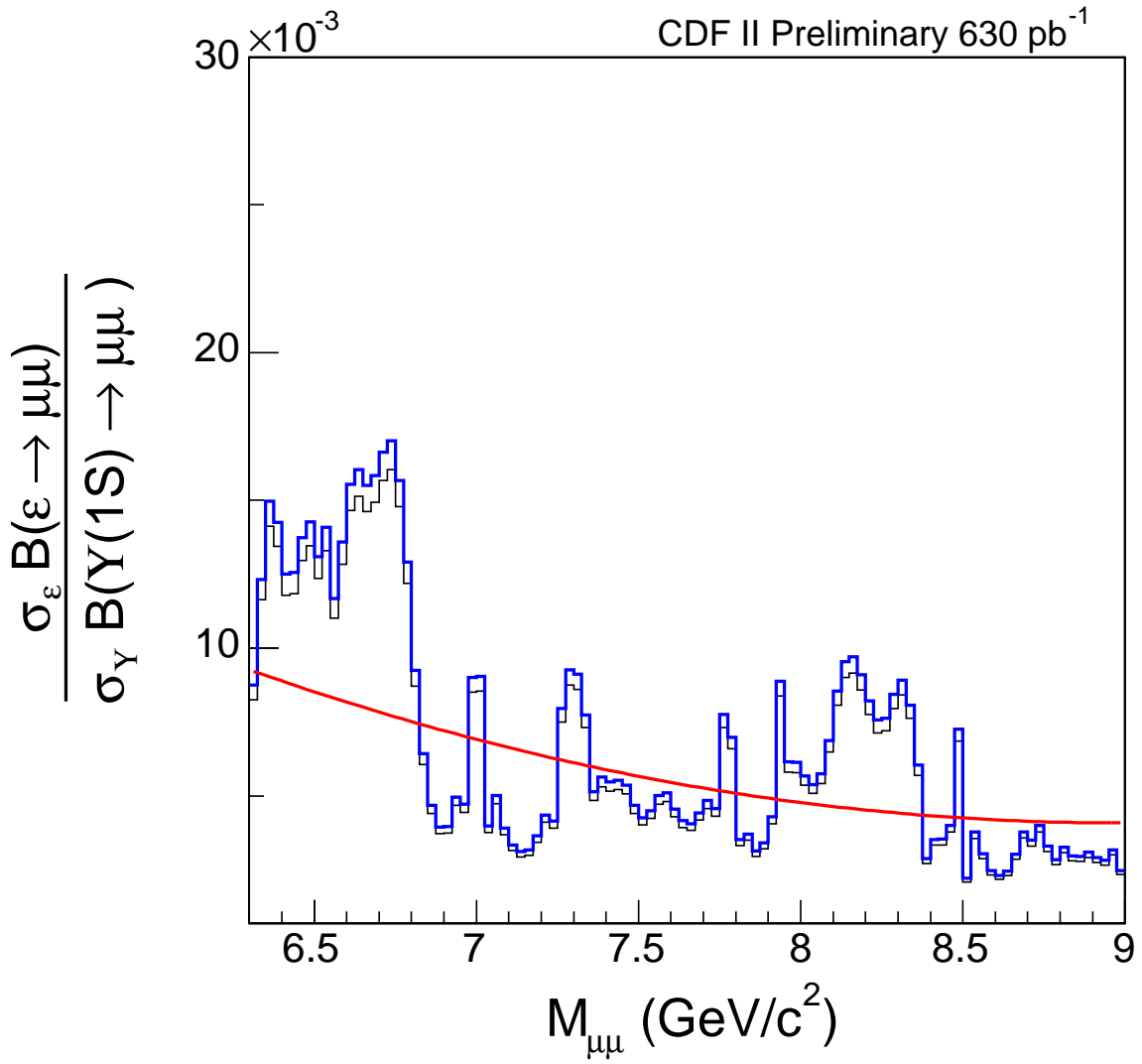


FIG. 2: Bayesian 90% upper credible limits to $\frac{\sigma_{\mathcal{E}} B(\mathcal{E} \rightarrow \mu\mu)}{\sigma_{\Upsilon(1S)} B(\Upsilon(1S) \rightarrow \mu\mu)}$ as a function of the \mathcal{E} mass.

90% upper credible limits to R , the ratio of the production cross section times muonic branching fraction of possible narrow resonances to that of the $\Upsilon(1S)$ meson. In this mass range, the average limit varies around 1%. Assuming that $\sigma_{\mathcal{E}} = \sigma_{\Upsilon(1S)} \times (m_{\Upsilon(1S)}/m_{\mathcal{E}})^3 \times \Gamma_{\mu}^{\mathcal{E}}/\Gamma_{\mu}^{\Upsilon(1S)}$, these limits correspond to an average 90% upper credible limit of less than 10 eV to the leptonic width of possible resonances. This results also indicates that the excess reported in [4] at a mass of 7.2 GeV/c² was a fluctuation.

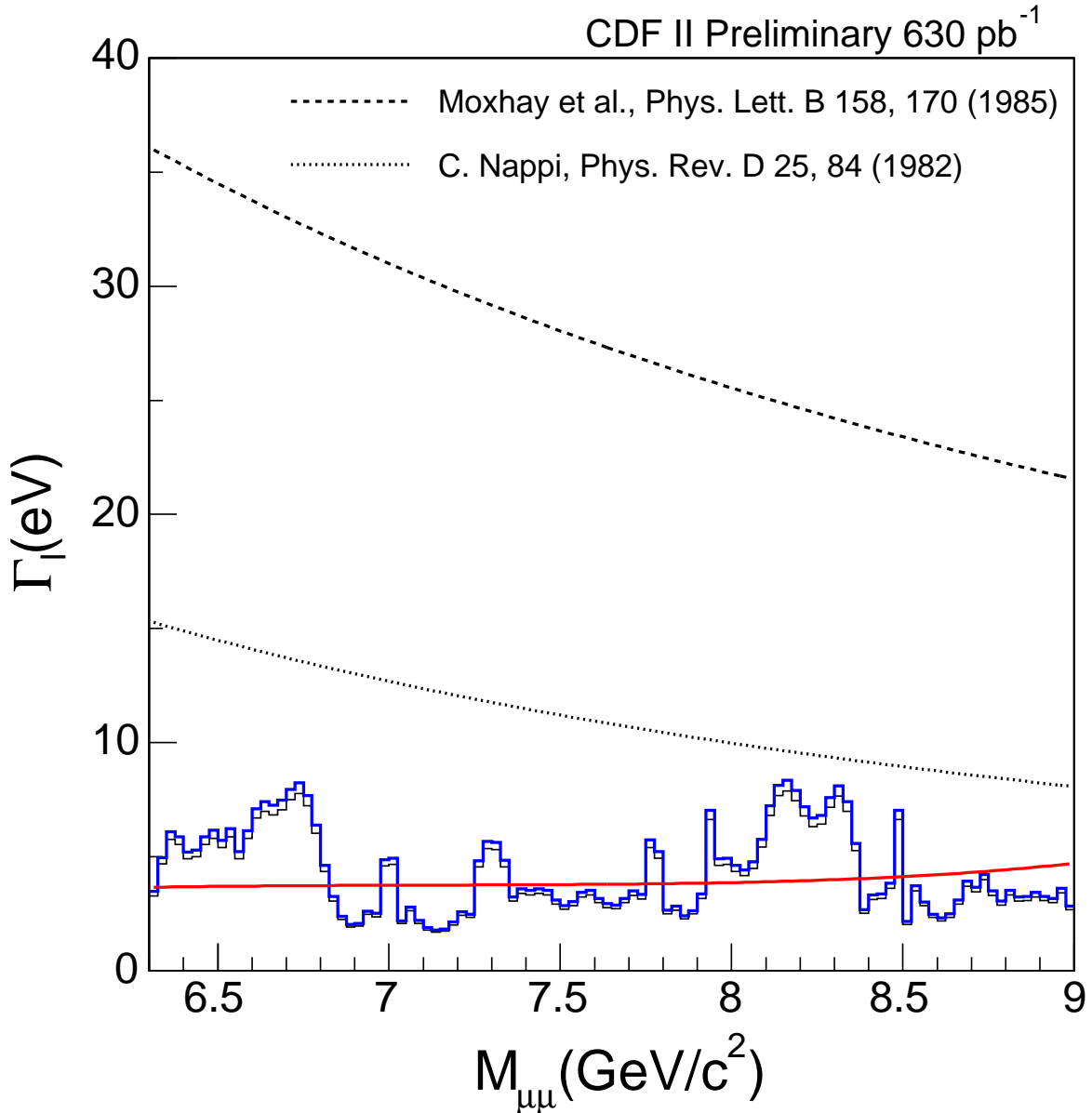


FIG. 3: Bayesian 90% upper limits to $\Gamma_l^{\mathcal{E}}$ (histogram). The dashed and dotted lines represent the leptonic widths of 1^{--} bound states of scalar quark predicted in Refs. [2] and [25], respectively.

VI. ACKNOWLEDGMENTS

We thank the Fermilab staff and the technical staffs of the participating institutions for their vital contributions. This work was supported by the U.S. Department of Energy and National Science Foundation; the Italian Istituto Nazionale di Fisica Nucleare; the Ministry

of Education, Culture, Sports, Science and Technology of Japan; the Natural Sciences and Engineering Research Council of Canada; the National Science Council of the Republic of China; the Swiss National Science Foundation; the A.P. Sloan Foundation; the Bundesministerium für Bildung und Forschung, Germany; the Korean Science and Engineering Foundation and the Korean Research Foundation; the Science and Technology Facilities Council and the Royal Society, UK; the Institut National de Physique Nucleaire et Physique des Particules/CNRS; the Russian Foundation for Basic Research; the Comisión Interministerial de Ciencia y Tecnología, Spain; the European Community's Human Potential Programme; the Slovak R&D Agency; and the Academy of Finland.

- [1] D. G. Aschman *et al.*, Phys. Rev. Lett. **39**, 124 (1977); A. M. Boyarsky *et al.*, Phys. Rev. Lett. **34**, 762 (1975); R. F. Schwitters in *Proceedings of the XVIII International Conference on High Energy Physics, Tbilisi* (1976), edited by N. N. Bogoliubov *et al.*, (JINR, Dubna, U.S.S.R. (1977).
- [2] C. Nappi, Phys. Rev. D **25**, 84 (1982).
- [3] T. Appelquist and H. D. Politzer, Phys. Rev. Lett. **34**, 43 (1975); E. Eichten *et al.*, Phys. Rev. D **17**, 3090 (1978).
- [4] G. Apollinari *et al.*, Phys. Rev. D **72**, 092003 (2005).
- [5] F. Abe *et al.*, Nucl. Instrum. Methods Phys. Res., Sect. A **271**, 387 (1988).
- [6] R. Blair *et al.*, Fermilab Report No. FERMILAB-Pub-96/390-E (1996).
- [7] C. S. Hill *et al.*, Nucl. Instrum. Methods Phys. Res., Sect. A **530**, 1 (2004).
- [8] A. Sill *et al.*, Nucl. Instrum. Methods Phys. Res., Sect. A **447**, 1 (2000).
- [9] T. Affolder *et al.*, Nucl. Instrum. Methods Phys. Res., Sect. A **453**, 84 (2000).
- [10] T. Affolder *et al.*, Nucl. Instrum. Methods Phys. Res., Sect. A **526**, 249 (2004).
- [11] G. Ascoli *et al.*, Nucl. Instrum. Methods Phys. Res., Sect. A **268**, 33 (1988).
- [12] J. Elias *et al.*, Nucl. Instrum. Methods Phys. Res., Sect. A **441**, 366 (2000).
- [13] D. Acosta *et al.*, Nucl. Instrum. Methods Phys. Res., Sect. A **461**, 540 (2001).
- [14] R. Downing *et al.*, Nucl. Instrum. Methods Phys. Res., Sect. A **570**, 36 (2007).
- [15] M. M. Block and R. N. Cahn, Rev. Mod. Phys. **57**, 563 (1985).
- [16] S. Klimenko *et al.*, Fermilab Report No. FERMILAB-FN-0741 (2003).

- [17] D. Acosta *et al.*, Phys. Rev. D **69**, 012002 (2004).
- [18] T. Aaltonen *et al.*, Phys. Rev. D **77**, 072004 (2008).
- [19] F. James and M. Roos, Comput. Phys. Commun. **10**, 343 (1975).
- [20] D. Acosta *et al.*, Phys. Rev. Lett. **88**, 161802 (2002); F. Abe *et al.*, Phys. Rev. Lett. **75**, 4358 (1995).
- [21] R. Brun *et al.*, CERN Report No. CERN-DD-78-2-REV; R. Brun *et al.*, CERN Programming Library Long Write-up W5013 (1993).
- [22] A. Abulencia *et al.*, Phys. Rev. D. **75**, 012010 (2007).
- [23] D. E. Acosta *et al.* [CDF Collaboration], Phys. Rev. Lett. **88**, 161802 (2002).
- [24] The D0 collaboration, arXiv:0804.2799, Fermilab Report No. FERMILAB-PUB-08-089-E, (2008).
- [25] P. Moxhay *et al.*, Phys. Lett. B **158**, 170 (1985).